Multichannel Cold Collisions: Simple Dependences on Energy and Magnetic Field

James P. Burke, Jr., Chris H. Greene, and John L. Bohn

JILA and Department of Physics, University of Colorado, Boulder, Colorado 80309-0440

(Received 8 June 1998)

The scattering matrices needed to describe cold collision processes are shown to have a simple dependence on energy and magnetic field, controlled by single-channel dynamics in the appropriate long-range field. A frame transformation describes the energy and field dependences entirely in terms of a standard recoupling matrix and single-channel parameters, giving adequate accuracy for many systems. The formulas in this paper should permit experimentalists to reproduce the results of hitherto complicated coupled channels calculations, through small, simple matrix manipulations. [S0031-9007(98)07406-7]

PACS numbers: 34.50.Pi, 32.80.Pj

Ultralow energy elastic and inelastic collisions play a crucial role in the theoretical description of Bose-Einstein condensates (BECs). Atom-atom scattering lengths control the rate of formation, the size, and to some extent the shape of single- and multiple-component condensates, while inelastic rate constants can control the trap lifetimes. The field-free scattering lengths are now known reasonably well for several alkali atom pairs, and many field-dependent scattering observables have been determined through fruitful collaborations between experiment and theory [1–3].

Moreover, the recent observation of Feshbach resonances in ^{23}Na [4] and ^{85}Rb [5] suggests the exciting possibility of a *tunable* effective interaction in BECs, and dramatizes the need for a simpler theoretical framework. Until now the theoretical community has primarily resorted to brute force numerical solutions of the multichannel close-coupling equations [1–3] in order to derive the relevant scattering information. The coupled equations are integrated out to internuclear distances R of order 10^3–10^4 a.u., for each collision energy E and magnetic field B of interest, which can become inordinately time and resource consuming.

The techniques of multichannel spectroscopy provide a powerful yet simple theoretical description of multichannel collisions and half-collisions, in contexts such as Rydberg electron motion [6] in the field of a structured ionic core. This approach has its origins in Seaton's [7] multichannel quantum defect theory (MQDT), and in multichannel effective range theory [8]. When suitably generalized to different long-range fields that arise in a two-body fragmentation channel, these methods can provide compact, quantitatively accurate theoretical descriptions of extremely complex observables.

This Letter presents a fully developed theoretical description of two-body ground state alkali-atom collisions. All of the system-specific scattering information at low energies is contained in a weakly energy-dependent short-range reaction matrix $\underline{K}^{\rm sr}$, which can be easily converted into physical quantum mechanical scattering amplitudes by manipulation of small matrices with the formulas presented below. The capability of MQDT formulations to describe multichannel observables relating to photoabsorption and collisions is well known, and it has already been applied to cold collisions by other groups [9–11]. Two key developments are described in this Letter: (i) A new *standardization of the long-range field properties* leads to a particularly compact representation of wave functions in the large-R region dominated by the usual multipole expansion. The long-range potential typically has the form $V^{\rm lr}(R) = -\frac{C_6}{R^6} - \frac{C_8}{R^8} - \frac{C_{10}}{R^{10}}$, but other long-range potentials can be similarly included, e.g., when retardation effects are important. (ii) A *recoupling frame transformation (FT)* approximation provides an adequate description of the physical scattering matrix $\underline{S}^{\rm phys}$ for many problems. When this approximation is valid, it permits a complete determination of $\underline{S}^{\rm phys}$ in terms of single-channel quantities (like singlet and triplet scattering phase shifts) and a standard angular momentum recoupling coefficient $X_{i\lambda}$.

Crucially, the frame transformation includes energetically closed channels as in previous MQDT studies [6], which distinguishes our FT from a related class of approximations (notably the degenerate internal states method [12], or equivalently the adiabatic nuclei method [13] of electron-molecule scattering theory). The strongest variations of the S matrix with E and B are associated with single-channel Schrödinger wave properties in the long-range field, or by Feshbach or shape resonances. These energy dependences emerge explicitly in terms of the standardized long-range field parameters identified under point (i) above.

In multichannel spectroscopy, the key idea is to express scattering observables in terms of a real, linearly independent base pair (f^0, g^0), which obey the radial Schrödinger equation in the long-range field, with boundary conditions chosen such that they are smooth, analytic functions of energy. A convenient, exact representation of (f^0, g^0) utilizes the amplitude $\alpha(R)$ in the Milne [14] phase-amplitude method [15]:

$$f^0(\varepsilon,l,R) = \sqrt{\frac{2\mu}{\pi}}\,\alpha(R)\sin\left(\int_{R_x}^{R}\frac{dR'}{\alpha^2(R')} + b_l\right),$$
$$g^0(\varepsilon,l,R) = -\sqrt{\frac{2\mu}{\pi}}\,\alpha(R)\cos\left(\int_{R_x}^{R}\frac{dR'}{\alpha^2(R')} + b_l\right). \quad (1)$$

The Milne amplitude $\alpha(R)$, which depends on l and on the energy ε, obeys a nonlinear differential equation, $\alpha''(R) + k^2(R)\alpha(R) = \frac{1}{\alpha^3(R)}$, where $k^2(R) \equiv 2\mu[\varepsilon - V^{\rm lr}(R) - \frac{l(l+1)}{2\mu R^2}]$. Application of WKB-style boundary conditions at some small fixed radius R_x (10 a.u. here), namely, $\alpha(R_x) = k(R_x)^{-1/2}$ and $\alpha'(R_x) = \frac{\partial}{\partial R_x}[k(R_x)^{-1/2}]$, is not "strictly necessary," but gives optimal smoothness [15] of $\alpha(R)$ in ε and R.

The *energy-independent* phase shift b_l in Eq. (1) is introduced here for the first time. It standardizes the low-energy asymptotic structure of (f^0, g^0) and simplifies the use of parameters calculated using different long-range potentials. This is useful, for instance, when collision properties must be calculated at many different values of the van der Waals coefficient C_6. Our new standardization of long-range solutions amounts to a choice of b_l such that $f^0(\varepsilon = 0, l, R) \to \text{const} \times R^{l+1}$, as $R \to \infty$. In the case of S-wave scattering, this amounts to demanding that the "comparison solution" $f^0(\varepsilon, l = 0, R)$ itself has *vanishing scattering length* in the limit $\varepsilon \to 0$. Unlike other quantum defect analyses [7,9–11,15], we have not specified the behavior of (f^0, g^0) at $R \to 0$. This is simply because (f^0, g^0) are never used there—they are used only to describe the large-R solutions, typically at $R \gtrsim 35$ a.u.

Standard multichannel scattering techniques integrate a set of $N = N_o = N_c$ coupled Schrödinger equations outward from the origin to some large internuclear distance $R_{\rm huge}$, where scattering boundary conditions are applied in the N_o open channels and exponential growth is eliminated in the N_c closed channels. We propose a simple modification: instead of integrating the coupled equations out to 10^4 a.u. where the long-range potential $V^{\rm lr}(R)$ is negligible, we now integrate them outward to a distance R_0 or order 30–60 a.u., beyond which exchange vanishes. The $N \times N$ solution matrix $\underline{M}(R)$ at a total energy E can then be written, in an asymptotic channel representation, as a linear combination of (f_i^0, g_i^0) at all radii $R \geq R_0$. Here f_i^0 and g_i^0 are diagonal matrices in the channel space, evaluated at the appropriate channel energy $\varepsilon_i = E - E_i$, where E_i is the dissociation threshold energy, and l_i is the relevant orbital momentum in the ith channel. N linearly independent solutions (regular at $R = 0$) that obey standing wave boundary conditions form the successive columns of $\underline{M}(R)$; beyond R_0, $\underline{M}(R)$ is characterized by a "smooth, short-range reaction matrix" $\underline{K}^{\rm sr}$ that varies slowly with E or B except near isolated poles. These N independent solutions are standardized to have the following form: $\underline{M}(R) = \underline{f}^0(R) - g^0(R)\underline{K}^{\rm sr}$, where $M_{ij}(R)$ is the ith channel component of the jth independent solution. The solution matrix still has components in energetically closed channels, but this method will usually work best if all channels included at $R \geq R_0$ are still "locally open," i.e., with $k^2(R) > 0$.

The representation of cold-collision properties presented in this paper can serve two different communities. First of all, it can be of use to theorists who want to speed up the solution of coupled equations, and who want to convey the maximum amount of information when tabulating results. Second, it can be useful to experimentalists and other theorists interested primarily in the low-energy scattering amplitudes for a range of E and/or B. Specifically, if theorists tabulate the short-range reaction matrix $\underline{K}^{\rm sr}$ at one energy, typically at a collision threshold, this is enough information to reconstruct many different scattering observables over a large range of E and B. The following steps are needed to extract the physical scattering matrix from such a tabulated matrix $\underline{K}^{\rm sr}$.

Step 1: Elimination of energetically closed channels.—Partition channels into N_o open channels (those channels $i \in P$, for which $\varepsilon_i = E - E_i > 0$) and N_c closed channels ($i \in Q$, for which $\varepsilon_i = E - E_i < 0$). In this notation, $\underline{K}^{\rm sr}$ becomes

$$\underline{K}^{\rm sr} = \begin{pmatrix} \underline{K}^{\rm sr}_{PP} & \underline{K}^{\rm sr}_{PQ} \\ \underline{K}^{\rm sr}_{QP} & \underline{K}^{\rm sr}_{QQ} \end{pmatrix}. \quad (2)$$

The exponentially growing parts of the wave functions at $R \to \infty$ are next "eliminated" in the MQDT sense, through the following equation which shows the potentially resonant influence of closed-channel pathways:

$$\underline{\tilde{K}} = \underline{K}^{\rm sr}_{PP} - \underline{K}^{\rm sr}_{PQ}(\underline{K}^{\rm sr}_{QQ} + \tan\underline{\beta})^{-1}\underline{K}^{\rm sr}_{QP}. \quad (3)$$

The resulting modified reaction matrix $\underline{\tilde{K}}$ has dimension $N_o \times N_o$. The diagonal matrix of closed-channel phase parameters $\beta = \int_{R_x}^{\infty} dR/\alpha^2(R) + b_l$ gives the coefficient [15] of the rising exponential for $f_i^0(R)$ (proportional to $\sin\beta_i$), and for $g_i^0(R)$ (proportional to $-\cos\beta_i$). Should all channels be closed, discrete bound states occur at roots of $\det(\underline{K}^{\rm sr}_{QQ} + \tan\underline{\beta}) = 0$.

Step 2: Transformation to an energy-normalized, nonanalytic long-range representation (f, g).—We ultimately desire a scattering solution normalized to $\delta(E - E')$. Three long-range field parameters $A, \mathcal{G}, \eta$ are relevant to this transformation, which can be written as

$$\begin{pmatrix} f(R) \\ g(R) \end{pmatrix} = \begin{pmatrix} A^{\frac{1}{2}} & 0 \\ -A^{\frac{1}{2}}\mathcal{G} & A^{-\frac{1}{2}} \end{pmatrix}\begin{pmatrix} f^0(R) \\ g^0(R) \end{pmatrix}. \quad (4)$$

At $R \to \infty$, (f, g) are phase shifted relative to spherical Bessel solutions:

$$f(R) \to kR\sqrt{2\mu/\pi k}\,[j_l(kR)\cos\eta - n_l(kR)\sin\eta],$$
$$g(R) \to kR\sqrt{2\mu/\pi k}\,[j_l(kR)\sin\eta - n_l(kR)\cos\eta], \quad (5)$$

with $k = \sqrt{2\mu\varepsilon}$. The standardized single-channel long-range field parameters $A(\varepsilon, l), \mathcal{G}(, l\varepsilon), \eta(\varepsilon, l)$ at $\varepsilon > 0$,

along with the phase $\beta(\varepsilon, l)$ at $\varepsilon < 0$, are calculated for the relevant long-range potential in each channel following the basic procedure described previously in Ref. [15], modified only by the new standardization condition above involving the constant shift b_l. In the following expressions, $\{\underline{A}, \underline{G}, \underline{\eta}\}$ are diagonal matrices in channel space. An $N_o \times N_o$ real, symmetric, "energy-normalized" reaction matrix in the (f, g) representation is obtained using [9]

$$\underline{K} = \underline{A}^{1/2}(\tilde{\underline{K}}^{-1} + \underline{G})^{-1}\underline{A}^{1/2}. \quad (6)$$

This is still not quite the "physical" reaction matrix $\underline{K}^{\rm phys}$ of conventional scattering theory owing to the phase shift $\eta(\varepsilon, l)$ of (f, g) relative to (j_l, n_l) at $R \to \infty$. Nevertheless, $\underline{K}$ possesses other properties expected in $\underline{K}^{\rm phys}$, such as the Wigner threshold behavior which is reflected in the dependence $A(\varepsilon, l) \sim \varepsilon^{l+1/2}$ as $\varepsilon \to 0$.

Step 3: Form the physical scattering matrix.—The final matrix manipulation needed is

$$\underline{S}^{\rm phys} = e^{i\underline{\eta}} \frac{1 + i\underline{K}}{1 - i\underline{K}} e^{i\underline{\eta}}. \quad (7)$$

From this expression, it is possible to extract inelastic scattering cross sections or rate constants, and elastic scattering cross sections, in the usual manner. When the scattering length in channel i is desired, it is the threshold limit $\varepsilon_i \to 0$ of the quantity $a_i = -(S_{ii}^{\rm phys} - 1)/2ik_i$, provided $l_i = 0$.

The long-range field parameters $A(\varepsilon, l)$, $G(\varepsilon, l)$, $\eta(\varepsilon, l)$, and $\beta(\varepsilon, l)$ can be tabulated once and for all as functions of the single parameter $\gamma = (2\mu)^3 C_6 \varepsilon^2$, in a.u. This scaling is *strictly* valid only for a pure van der Waals long-range potential, but in practice it still holds to a good approximation even for the above form of $V^{\rm lr}(R)$ with additional C_8 and C_{10} terms. Our standardization of the zero-energy scattering length of $f^0(r)$ leads to one major benefit: the long-range parameters are almost independent of the C_8, C_{10} terms. When tabulated as functions of the parameter γ they are nearly atom independent for the cases we have explored numerically (see the inset of Fig. 1). Additional details about these parameters will be published separately, but for now a table for their values sufficient to reproduce, e.g., the S-wave scattering calculations shown in this paper, can be found in Ref. [16].

We have verified that no accuracy is lost in calculated elastic and inelastic cross sections when the multichannel solutions are represented beyond $r = r_0$ by the semianalytic long-range reference functions (f_i^0, g_i^0), rather than by brute force numerical solution. More to the point, the resulting calculated reaction matrix $\underline{K}^{\rm sr}$ hardly changes over an energy range of 10–100 mK. The reader interested in seeing an implementation of the quantum defect calculation can find in Ref. [16] a MATHEMATICA notebook that implements steps 1–3 above for an energy-independent $\underline{K}^{\rm sr}$ matrix for ^{85}Rb-^{85}Rb, and reproduces Fig. 1.

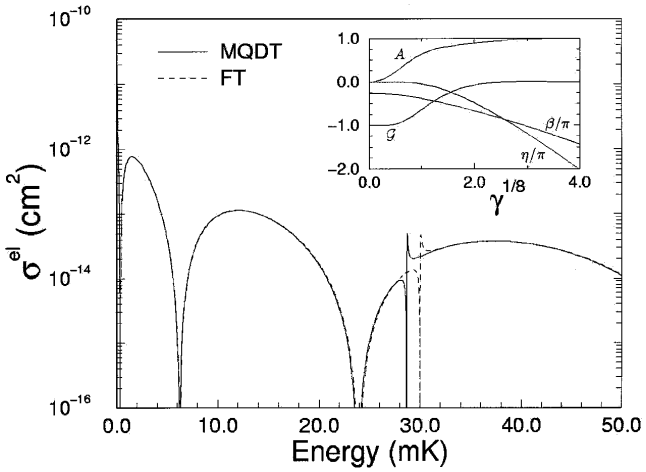

FIG. 1. Elastic S-wave partial cross section for the collision of two ^{85}Rb atoms in their $|2, -2\rangle$ atomic hyperfine states. The feature near 29 mK is the zero-field version of the Feshbach resonance [5]. Solid curve: an MQDT calculation using a constant $\underline{K}^{\rm sr}$, which is indistinguishable on this scale from a highly accurate FEM R-matrix calculation. Dashed line: the FT approximation. Inset: The four long-range QDT parameters, as functions of the parameter γ defined in the text, which coincide on this scale for identical-atom collisions of Na, K, or Rb.

Figure 1 shows a calculation of the S-wave elastic scattering cross section σ^{el} for two ^{85}Rb atoms in the same $|f_a m_a\rangle = |f_b m_b\rangle = |2, -2\rangle$ atomic hyperfine states. The solid line represents the cross section calculated with a *constant* short-range reaction matrix $\underline{K}^{\rm sr}$ via steps 1–3 above. It is indistinguishable from the "essentially exact" cross section derived from a finite element (FEM) [17] R-matrix [6] solution of the coupled Schrödinger equations, as implemented in our previous work [3]. The MQDT results quantitatively reproduce *all* features of this spectrum, with a $\underline{K}^{\rm sr}$ computed from the coupled equations at the *single* energy $E = 0$. This excellent agreement over an extended energy range confirms that $\underline{K}^{\rm sr}$ is weakly energy dependent. The calculation using a constant $\underline{K}^{\rm sr}$ matrix also predicts the energy of the zero-field Feshbach resonance [5] (near 30 mK) to within 0.1 mK. The small shift in the resonance position indicates that $\underline{K}^{\rm sr}$ is not strictly constant over this energy range. Effects associated with this slight energy dependence can be incorporated by interpolation of $\underline{K}^{\rm sr}$ after it is tabulated on a coarse energy grid. (See Ref. [6] for a discussion of practical considerations relevant to such interpolations.) Figure 1 exemplifies the usefulness of tabulating results in terms of $\underline{K}^{\rm sr}$. Whereas the zero-energy scattering length a provides a useful approximation for the elastic scattering cross section $\sigma = 8\pi a^2$ only for collision energies below $E \sim 1\ \mu$K in ^{85}Rb, the short-range reaction matrix $\underline{K}^{\rm sr}$ provides quantitative information over tens of mK, the entire range relevant to cold collision physics.

The theory presented above still requires integration of coupled channel equations to obtain $\underline{K}^{\rm sr}$. However, in

cold alkali collisions the dominant spin exchange coupling interaction is localized in the range $R \sim 25$ a.u. To a good approximation the atoms move at $R \lesssim 20$ a.u. in a set of uncoupled channels, labeled by their total electronic spin quantum number S. We thus integrate the *single-channel* Schrödinger equations with all hyperfine interactions *omitted*, and then match each solution to the energy-analytic base pair (f^0, g^0) to obtain singlet $(S = 0)$ and triplet $(S = 1)$ quantum defects $\mu_S^{\rm sr}(\varepsilon)$. The short-range reaction matrix is then approximated by the energy-dependent frame transformation formula

$$K^{\rm sr}_{i,i'} = \sum_\lambda \langle i|\lambda\rangle \tan \pi \mu^{\rm sr}_\lambda(\overline{\varepsilon}_\lambda) \langle \lambda|i'\rangle . \qquad (8)$$

Here $X_{i\lambda} = \langle i|\lambda\rangle$ represents the (symmetrized) unitary transformation matrix that connects the short-range basis $|\lambda\rangle \equiv |(s_a, s_b)S(i_a, i_b)IFM\rangle$ with the asymptotic hyperfine basis $|i\rangle \equiv |(s_a, i_a)f_a(s_b, i_b)f_bFM\rangle$. In a different implementation of the energy-dependent FT than used previously, we choose $\overline{\varepsilon}_\lambda$ to be a weighted average of the channel energies ε_i appropriate for eigenchannel $|\lambda\rangle$, namely, as $\overline{\varepsilon}_\lambda \equiv \sum_i \varepsilon_i |\langle i|\lambda\rangle|^2$. Finally, steps 1–3 above determine $\underline{S}^{\rm phys}$. (A qualitative analysis having some features in common with our FT was recently proposed [18]. In that work, however, the $\underline{R}$ matrix was transformed at a specific radius, rather than $\underline{K}^{\rm sr}$, which is less accurate because $\underline{R}$ is more energy dependent than $\underline{K}^{\rm sr}$.)

The FT approximation in Fig. 1 reproduces the energy dependence of the ^{85}Rb elastic cross section over 50 mK, except for an error of $\sim$1.4 mK in the zero-field Feshbach resonance energy. The FT differs from our "exact" FEM R-matrix results by less than 2% at $E = 50$ mK. In tests conducted for calculations of inelastic rates, the FT seems to remain quite accurate, except when destructive interference reduces their values to less than $\sim 10^{-13}$ cm^3/sec, as in ^{87}Rb.

The energies and widths of Feshbach resonances that arise in the presence of an applied magnetic field are also predicted by this approximation. A straightforward generalization of the FT (8), which includes the additional rotation into asymptotic dissociation channels obtained by diagonalizing the atomic Zeeman Hamiltonian, predicts the Na and Rb resonances observed [4,5], at magnetic field values within 5% of their more accurate FEM R-matrix resonance positions, and with comparable widths. Still better results emerge if a constant coupled-channel K matrix determined at $B = 0$ and at lowest hyperfine threshold is used, without resorting to the $\langle f_a f_b|SI\rangle$ FT [Eq. (8)]: The field values of the ^{23}Na resonances (853 G, 907 G), and of the ^{85}Rb resonances (164 G [5]), are in error (relative to FEM R matrix) by less than 2%. We stress that essentially exact agreement with the FEM calculations are obtained if $\underline{K}^{\rm sr}$ is interpolated versus B. [It may be of interest that, for ^{23}Na, the difference between elastic ^{23}Na scattering lengths for $f_a = 1, f_b = 1$ collisions is $a(F = 2) - a(F = 0) \simeq 5.3$ a.u., while their average is $\simeq$52 a.u., after the Na potentials are revised to achieve consistency with the resonance positions observed by Ref. [4].]

In summary, we have presented a fully developed MQDT theory applicable to cold collisions of alkali atoms that improves upon existing techniques by orders of magnitude in efficiency. The theory parametrizes the main energy and field dependences of $\underline{S}^{\rm phys}$, in terms of four "standard" long-range MQDT parameters A, $\mathcal{G}$, η, and β. The last quantity required, $\underline{K}^{\rm sr}$, contains the entire multichannel nature of the physics, but depends weakly on energy and field. In many cases $\underline{K}^{\rm sr}$ is represented solely in terms of single-channel parameters plus a recoupling matrix, while still producing quantitative results. The treatment yields similar efficiency gains when implemented for photoassociation calculations.

We acknowledge support from the National Science Foundation, and helpful discussions with M. Cavagnero, Bo Gao, F. Mies, and M. Raoult.

[1] P. S. Julienne *et al.,* Phys. Rev. Lett. **78**, 1880 (1997).
[2] H. M. J. M. Boesten *et al.,* Phys. Rev. A **55**, 636 (1997).
[3] J. P. Burke, Jr. *et al.,* Phys. Rev. A **55**, R2511 (1997).
[4] S. Inouye *et al.,* Nature (London) **392**, 151 (1998).
[5] Ph. Courteille *et al.,* Phys. Rev. Lett. **81**, 69 (1998).
[6] M. Aymar *et al.*, Rev. Mod. Phys. **68**, 1015 (1996).
[7] M. J. Seaton, Rep. Prog. Phys. **46**, 167 (1983).
[8] C. M. Lee, Phys. Rev. A **11**, 1692 (1975).
[9] F. H. Mies, J. Chem. Phys. **80**, 2514 (1984); F. H. Mies and P. S. Julienne, J. Chem. Phys. **80**, 2526 (1984); M. Raoult and F. H. Mies, in *Proceedings of the XIX ICPEAC Meeting, Scientific Program and Abstracts of Contributed Papers,* edited by J. B. A. Mitchell, J. W. McConkey, and C. E. Brion (1995), p. 626; F. H. Mies and M. Raoult (unpublished).
[10] B. Gao, Phys. Rev. A **54**, 2022 (1996); B. Gao, Phys. Rev. A (to be published).
[11] M. J. Cavagnero, Phys. Rev. A **50**, 2841 (1994); M. J. Cavagnero (unpublished).
[12] H. T. C. Stoof *et al.,* Phys. Rev. B **38**, 4688 (1988).
[13] D. M. Chase, Phys. Rev. **104**, 838 (1956); R. K. Nesbet, Comments At. Mol. Phys. **11**, 25 (1981); H. Gao and C. H. Greene, J. Chem. Phys. **91**, 3988 (1989), and references therein.
[14] W. E. Milne, Phys. Rev. **35**, 863 (1930).
[15] B. Yoo and C. H. Greene, Phys. Rev. A **34**, 1635 (1986); see also C. H. Greene *et al.,* Phys. Rev. A **26**, 2441 (1982), Sect. IVB.
[16] http:/condon. colorado.edu/∼chg/Collisions
[17] J. P. Burke, Jr. *et al.,* Phys. Rev. A **54**, 3225 (1996).
[18] J. M. Vogels *et al.,* Phys. Rev. A **57**, 4049 (1998).